Evaluative study on the interactive ability of phenolic acids derived from Pomegranate peel with Cu^{2+} ions as examined using UV-Vis spectroscopy

How do phenolic acid derivatives obtained from pomegranate peel interact with copper (II) ions as investigated using UV-Visible Spectroscopy?

Word Count: 3931

Table of Contents

1 Abbreviations Chart

Abbreviation	Explanation
PP	Pomegranate peel
PPP	Pomegranate peel powder
EDTA	Ethylenediaminetetraacetic acid
GA	Gallic acid
EA	Ellagic acid
EI	Extent of interaction
CuSO$_4$	Copper (II) sulfate
Cu	Copper

2 Introduction and Rationale

Ensuring access to clean water for everyone is one of the UN's Sustainable Development Goals *(United Nations)*. Nearly 800 million people worldwide lack reliable access to clean drinking water *(Water.org)*. Unequal access to clean drinking water is estimated to cost the world around $260 billion USD annually *(Water.org)*. One of the main causes for the contamination of water is due to wastewater effluent from factories which dangerously increase the amount of heavy metals such as copper (Cu) in the waterways *(Mokarram, Saber and Sheykhi)*. The deleterious effects of heavy metal poisoning of drinking water are well documented and known - heavy metal contamination can lead to the development of several critical health conditions *(Rehman, Fatima and Waheed)*.

Addressing this contamination requires effective remediation methods. The conventional Ethylenediaminetetraacetic acid (EDTA) filtering method for remediating heavy metal contaminated water that was taught in Chemistry class is efficient (due to its hexadentate nature) but EDTA's resistance to bacterial biodegradation *(Hinck, Ferguson and Puhaakka)* and the adverse effects of its complexes *(Crisponi, Nurchi and Lachowicz)* nullifies its effectiveness in today's eco-conscious world. Hence research has been undertaken in order to find alternate organic sources of chelating agents *(Rashed and Tayh)*.

One such promising avenue for green alternatives to EDTA is pomegranate peels (PPs). Pomegranates are enjoyed by many across the world, thanks to their taste and numerous health benefits *(Zarfeshany, Asgary and Javanmard)*. 2.5-3 million tons are produced annually and are used in various industries such as in the beverage and food industry *(Görgüç, Gençdağ and Yılmaz)*. However, PPs, which consist of approximately 30% of the whole fruit's weight *(Mo, Ma and Gao)*, are generally discarded, even though they have been identified as a valuable reservoir of organic polyphenolic substances such as tannins, flavonoids, and phenolic acids (Figure 1).
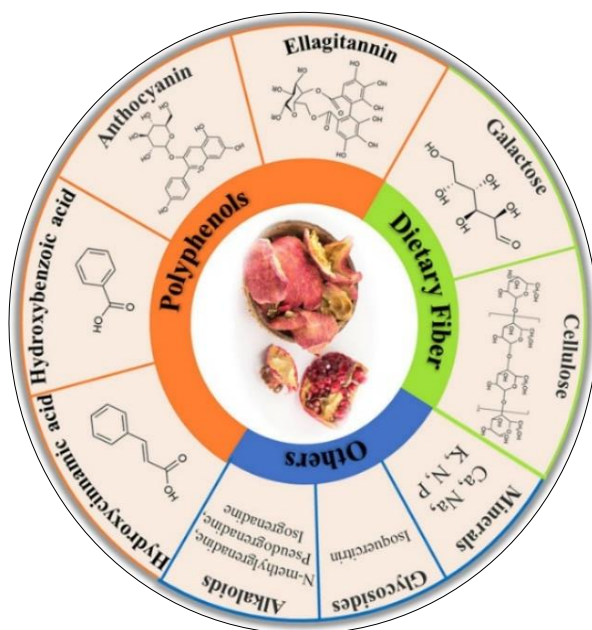
Figure 1: Some bioactive compounds present in PPs (Mo, Ma and Gao)

These polyphenols consist of up to 50% of the weight composition of PPs (depending on the extraction method and testing method used) *(Mo, Ma and Gao)*. This high polyphenolic content makes PPs a promising green alternative to traditional chelating agents for treating heavy metal contaminated water as they have been known to effectively interact with heavy metal ions such as Cu *(Rashed and Tayh)*.

Hence, the present study aims to explore the mechanism of the interaction between the polyphenols offered by the PP and the Cu ions.

3 Research Question

This led me to formulate the research question for the study – **How do phenolic acid derivatives obtained from pomegranate peel interact with copper (II) ions as investigated using UV Visible Spectroscopy?**

The study explores the optimal mass of pomegranate peel powder (PPP), solvent of extraction, Cu ion concentration, metal-ligand ratio, and pH environment which yields the highest extent of interaction (EI). UV-Visible spectrophotometry employs an empirical role

in understanding the interactions that take place between the phenolic derivatives and the Cu^{2+} ions. Before investigating the details of these interactions, we need to look into the individual components first.

4 Background Information

4.1 Copper
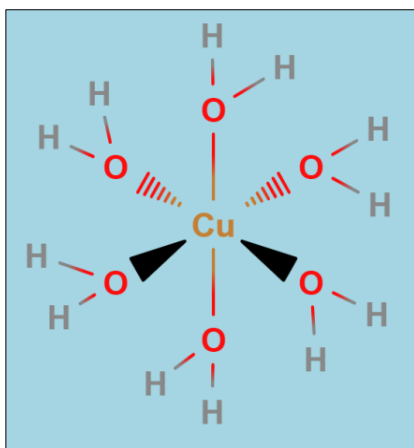
Figure 2: The octahedral structure of the complex [Cu(H₂O)]₆]²⁺ (Hexaaquacopper (II)) (MolView)

The metal ion, Cu^{2+}, takes up the central point of the interaction and is the third most used metal in industries such as wiring and construction *(U.S. Congress, Office of Technology Assessment)*. Water is the primary medium through which it enters into the body *(Manne, Kumaradoss and Iska)*.

Located in the d-block of the periodic table, Cu is a transition metal with a unique electronic configuration of

$[Ar]4s^13d^{10}$. This configuration is taken by the Cu atom as it is more stable having a partially filled s-orbital than an incompletely filled d-orbital *(Brown and Ford)*. Cu can exist in two oxidation states including as Cu^+, however, the most common state is Cu^{2+} with the loss of one electron from the outermost 4s-subshell and the loss of another electron from the 3d-subshell. In its more stable +2 oxidation state, Cu ions have a maximum of six binding sites as depicted in Figure 2. These binding sites allow molecules called ligands to form coordinate bonds with the Cu ion, forming Cu complexes.

4.2 Ligands and Denticity

As briefly outlined in the previous section, ligands are molecules or ions that bind to a central metal ion to form a substance called a complex , with the polyphenolic derivatives from PP being the ligands used in this study. Ligands have one or more pair of electrons that can form

one or more dative bonds with a metal ion. They act as a Lewis base through electron pair donation, while the metal ion acts as a Lewis acid via accepting them.

Ligands are classified by two factors, their denticity and strength. Denticity is a characteristic of a ligand's binding site(s). For example, as seen in Figure 3, when a polydentate ligand approaches a metal ion, multiple dative bonds are formed between the metal ion and the binding sites of the ligand. This process is a special type of complexation called chelation.

4.3 Chelation

Figure 3: Pictorial representation of complexation (top) and chelation (bottom) (Flora and Pachauri)
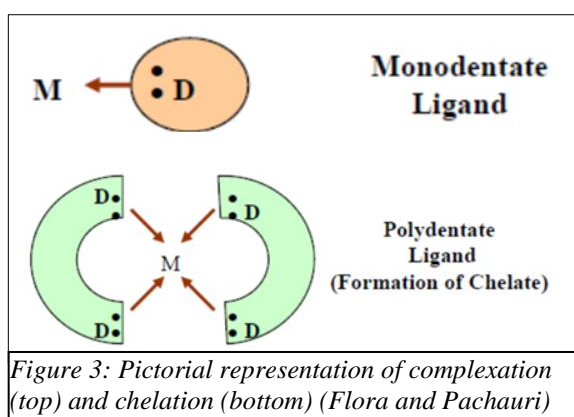
Chelation differs from complexation by the denticity of the participating ligands. Monodentate ligands like water offer only one binding site, leading to complexation as seen in Figures 2 and 3.

Chelating agents wrap around the metal ion, forming ring-like/cage-like structures called chelate complexes or chelates which boost the stability of the complex - this is referred to as the chelate effect *(Lancashire)*. Chelation is the primary type of interaction that takes place between the Cu^{2+} ions and the phenolic derivates from the PP as will be detailed in the following sections.

Another factor used to categorize ligands is their strength (as mentioned in the Section 4.2), which will be detailed upon in the following section.

4.4 Ligand Strength and Colored Complexes

When the ligands interact with a metal ion, the degeneracy (energy-level) of the metal ion's d-orbital is lifted, resulting in the formation of t_{2g} and e_g sub-levels. The energy difference between these sub-levels is influenced by the properties of both the metal ion and the ligand.

This determines the wavelength of light which is absorbed by the complex, thus resulting in the complementary color being seen. This process is visually detailed in Flowchart 1.
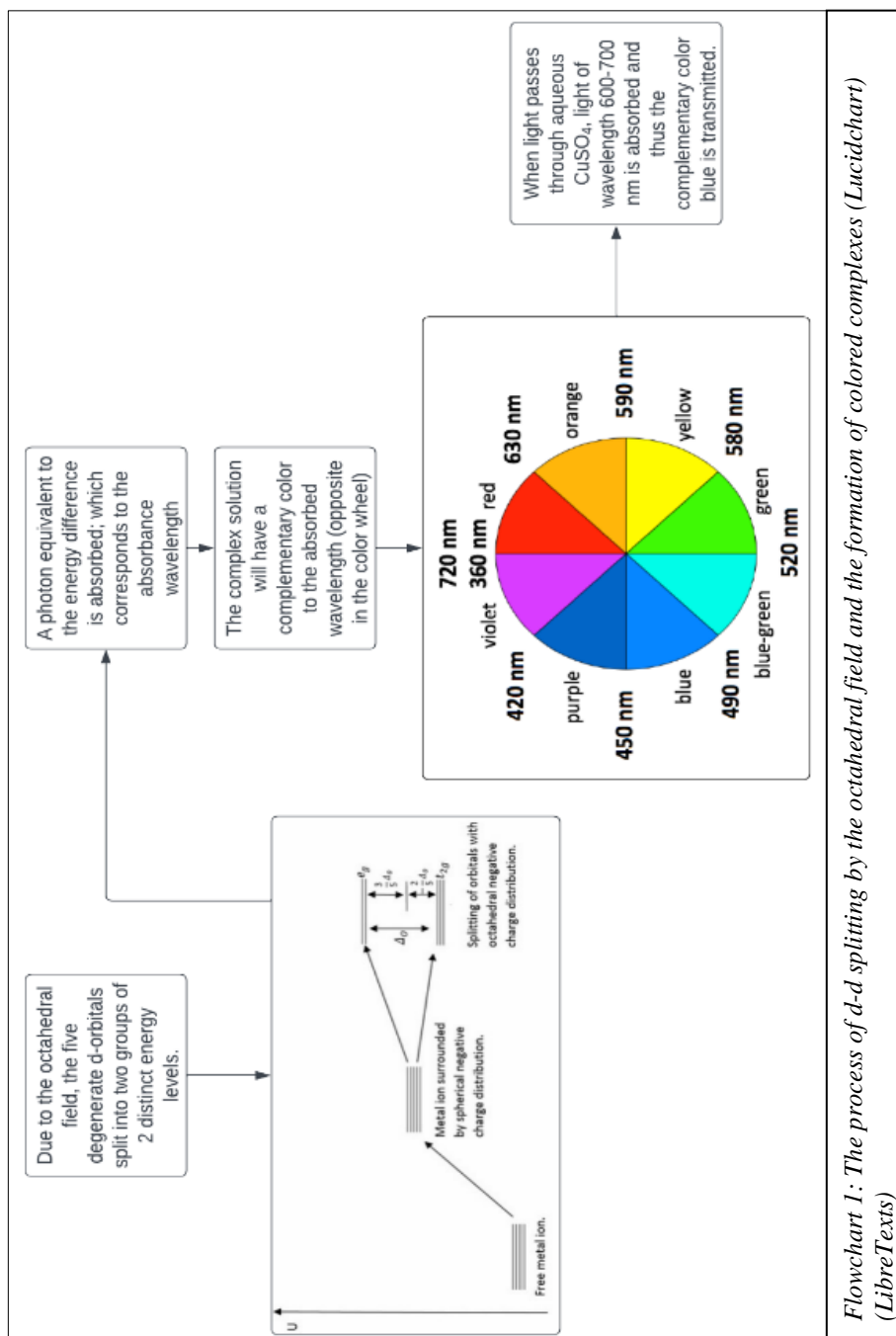
Flowchart 1: The process of d-d splitting by the octahedral field and the formation of colored complexes (Lucidchart) (LibreTexts)

Given that the function of the polyphenolic derivates from PP as chelators is now established, it is reasonable to delve deeper into the specificities of these chelate-metal ion interactions – first, however, this requires an understanding of the polyphenolic profile of PPs.

4.5 Polyphenols present in PP

Phenolic compounds, such as polyphenols, are a major group of compounds recognized for their contribution to our health *(Belščak-Cvitanović, Durgo, and Huđek)*. They are characterized by the presence of multiple phenol groups in the molecule, making them effective natural metal chelating agents as identified in literature *(Belščak-Cvitanović, Durgo, and Huđek)*.

The primary polyphenols identified in PPs are gallic acid (GA) and ellagic acid (EA) (which constitute approximately 60-80% of the total phenolic content depending on the extraction conditions) (Figure 4). Specifically, GA and EA are present in a ratio of 1:3 (Figure 4). Other polyphenols present in large quantities in PPP extracts include flavonoids such as catechin and epicatechin (Figure 4).

Content (µg/g ± SD)		UE			SE	CM
		MeOH	EtOH	Ace	Ace	Ace
Flavonoids	Catechin	169.37 ± 5.45	78.14 ± 2.69	121.73 ± 2.11	60.84 ± 2.79	246.73 ± 4.83
	Epicatechin	989.13 ± 16.02	350.74 ± 5.55	510.01 ± 14.79	1594.62 ± 69.77	433.64 ± 12.90
	Hesperidin/Neohesperidin	8.85 ± 0.95	22.34 ± 1.05	44.76 ± 1.98	11.20 ± 0.68	41.51 ± 2.11
	Rutin	9.34 ± 0.56	23.65 ± 1.71	54.39 ± 2.44	8.25 ± 1.15	87.02 ± 5.80
Phenolic acids	Caffeic acid	16.25 ± 1.59	12.24 ± 2.55	28.44 ± 1.63	20.33 ± 1.89	18.21 ± 2.00
	Chlorogenic acid	1.33 ± 0.02	2.03 ± 0.03	5.53 ± 0.05	8.41 ± 0.10	2.37 ± 0.02
	Ellagic acid	4585.77 ± 222.12	4798.66 ± 198.25	6883.41 ± 111.89	6377.43 ± 291.11	5601.08 ± 211.87
	Gallic acid	4256.04 ± 187.45	1652.95 ± 52.49	2656.32 ± 105.30	3396.03 ± 99.58	1018.71 ± 20.98
Total content of analyzed polyphenols		10036.08 ± 434.16	6940.74 ± 264.32	10304.60 ± 240.19	11477.11 ± 467.07	7449.26 ± 260.51

Results are expressed as µg of component/g of extract. All experiments were conducted in triplicates and results are reported as a mean ± SD.

Figure 4: Chemical constituents of PPP extracts in varying extraction conditions (Kupnik, Leitgeb and Primožic)

The molecular structures of GA and EA are shown in Figures 5 and 6 below. As seen in the structures, both phenols have multiple hydroxyl groups, with GA having a carboxylic group as well. These groups can donate electrons to the Cu^{2+} ions.

Figure 6: Molecular structures of two major polyphenolic constituents of PP, GA and EA (MolView)

Figure 5: Molecular structures of two minor polyphenolic constituents of PP (MolView)
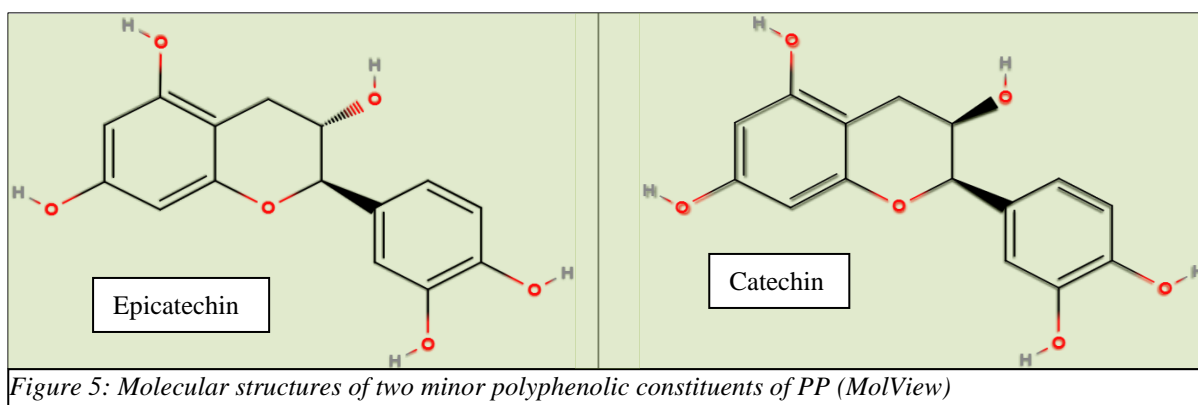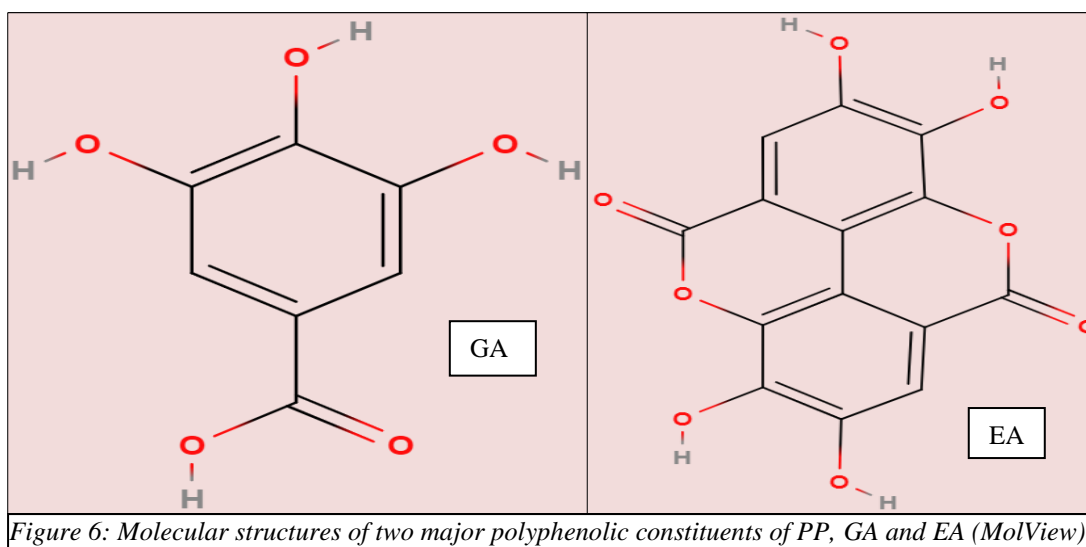
GA should be considered a bidentate ligand that can only bind with a singular Cu ion. EA, on the other hand, can undergo chelation with Cu as it has four hydroxyl groups. This is because GA can only undergo complexation as the oxygen atom in the central hydroxyl group (Figure 5) cannot form multiple dative bonds while the hydroxyl groups in EA (Figure 5) are free to coordinate with Cu independently.

These two ligands, along with other polyphenols present in PPP extract as elaborated in Figure 4, contribute to the PP's ability to treat heavy metal contaminated water.

4.6 Possible Complex Formations

The bidentate and polydentate nature of GA and EA respectively enables the formation of a variety of Cu-ligand complex structures. Probable structures are shown below in Figures 7

and 8 respectively. It should be noted that, in Figure 8, the Cu-EA complexes can form long-chain complexes since the Cu ions in the periphery of the EA molecules could coordinate with neighboring EA or even GA or other ligand molecules. Moreover, these long-chain complexes should have greater stability (Section 4.3), increasing the chances for their formation (although there is the issue of steric hindrance caused by the large ligand molecules surrounding the Cu).

Figure 7: Possible Cu-GA complexes. (MolView)

Figure 8: Possible Cu-EA complexes. (MolView)
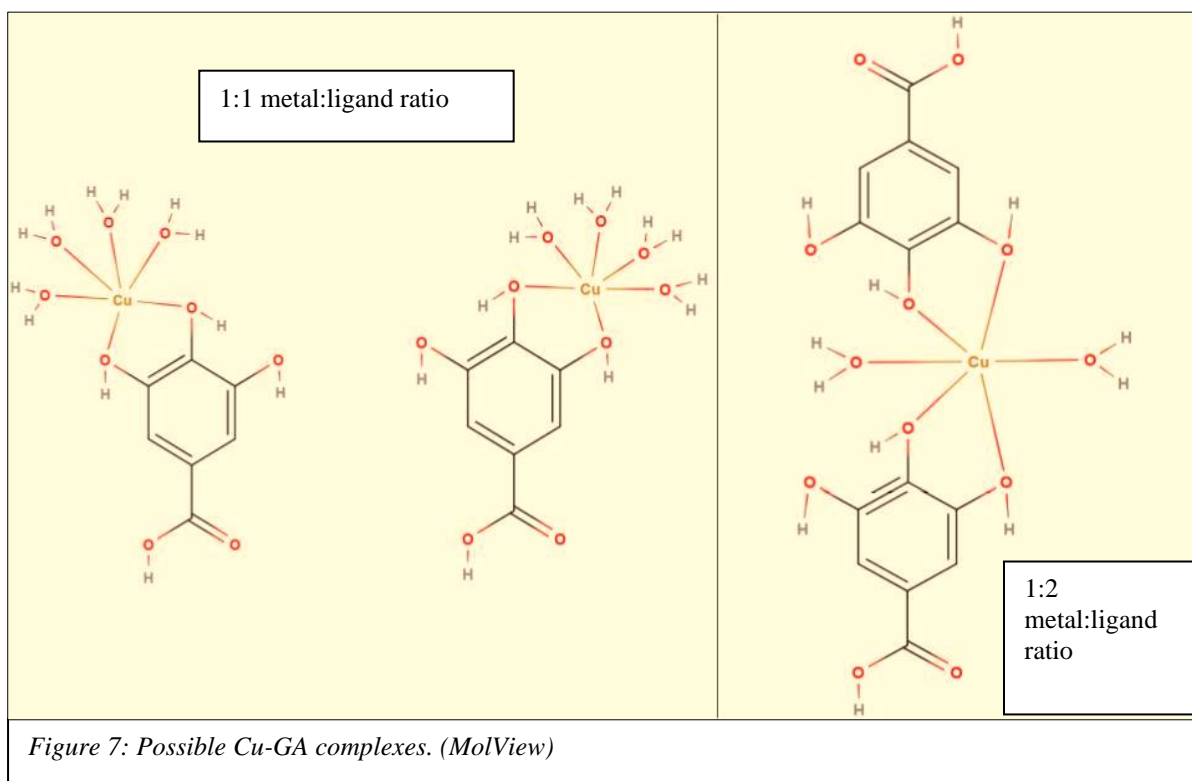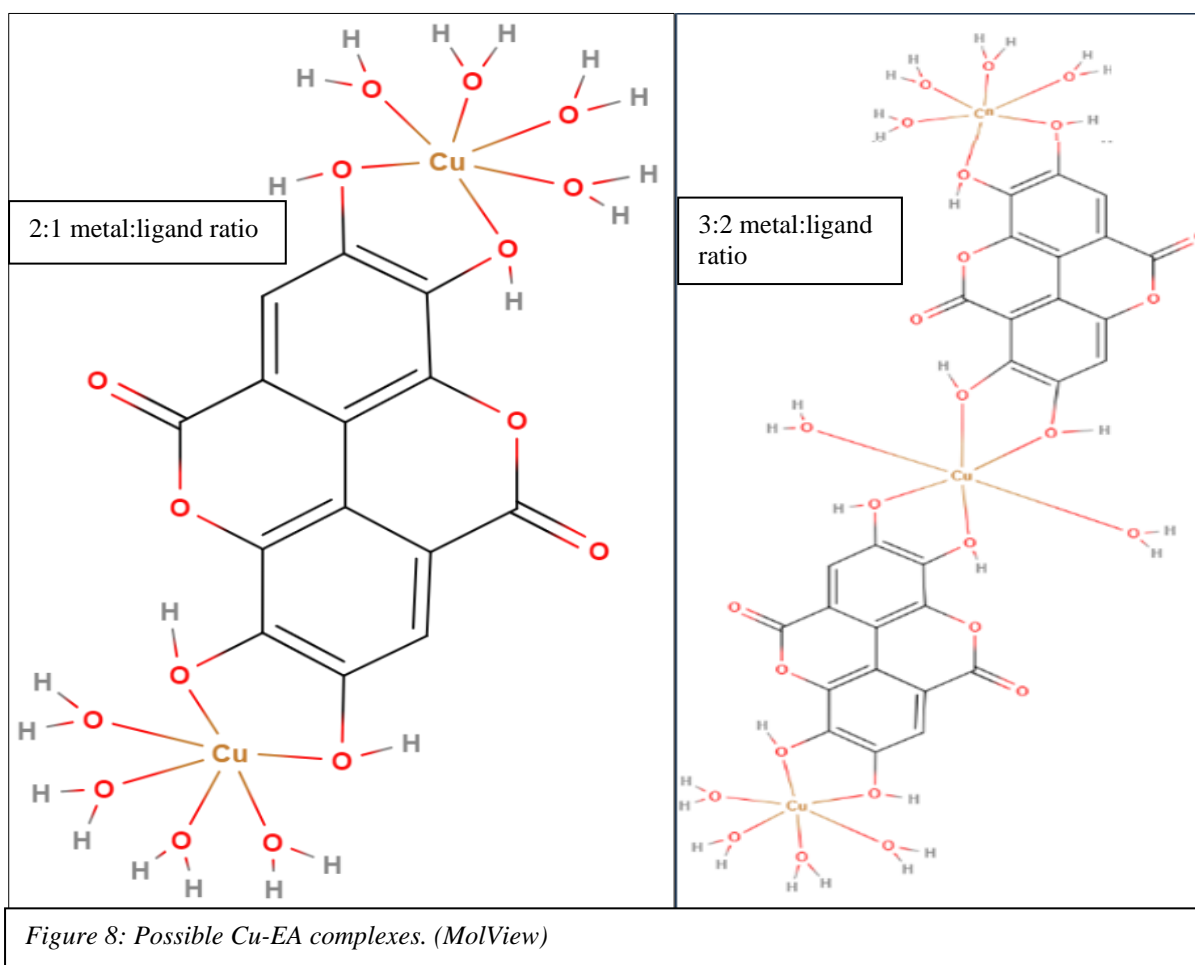
A point to note is that polyphenols are known to reduce Cu^{2+} ions to Cu^+ *(Akagawa and Suyama)*. However, the extent to which this occurs is negligible in normal complexation conditions *(Akagawa and Suyama)*.

Furthermore, it is important to understand the thermodynamics behind the interaction between the ligands and Cu since it is the driving force behind the extent of complexation.

4.7 Thermodynamics in Chelation

The thermodynamic properties of two reactions will be examined – the formation of a Cu-hydrated complex from $CuSO_4$ and the formation of Cu-GA and Cu-EA complexes.

$\Delta H_{\text{lat}}(\text{CuSO}_4) = 3066\text{kJ}$ *(Yoder and Flora)*

$\Delta H_{\text{hyd}}(\text{Cu}^{2+}) = -2100 \text{ kJmol}^{-1}$ *(Chieh)*

$\Delta H_{\text{hyd}}(\text{SO}_4^{2-}) = -1099 \text{ kJmol}^{-1}$ *(Barret)*

$$\Delta H_{\text{hyd}}(\text{CuSO}_4) = \left|\Delta H_{\text{hyd}}(\text{Cu}^{2+}) + \Delta H_{\text{hyd}}(\text{SO}_4^{2-})\right|$$

$$\Delta H_{\text{hyd}}(\text{CuSO}_4) = |(-2100) + (-1099)|$$

$$\Delta H_{\text{hyd}}(\text{CuSO}_4) = 3199\text{kJ}$$

$$\mathbf{\Delta H_{\text{hyd}}(\text{CuSO}_4) > \Delta H_{\text{lat}}(\text{CuSO}_4)}$$

Hence this drives the solvation of Cu ions by water molecules and the formation of Cu-hydrated complexes such as Hexaaquacopper (II) (Figure 2) *(Clark)*.

$$[\text{Cu}(\text{H}_2\text{O})_6]^{2+} + \text{GA} \rightarrow [\text{CuGA}(\text{H}_2\text{O})_4]^{2+} + 2\text{H}_2\text{O} \quad (\Delta S = +\text{ive})$$
$$[\text{Cu}(\text{H}_2\text{O})_6]^{2+} + 2\text{GA} \rightarrow [\text{Cu}(\text{GA})_2(\text{H}_2\text{O})_2]^{2+} + 4\text{H}_2\text{O} \quad (\Delta S = +\text{ive})$$
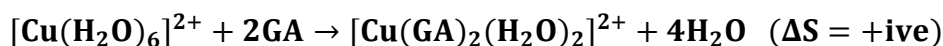
Equation 1: Represents complexation reactions from Figure 7.

$$2[\text{Cu}(\text{H}_2\text{O})_6]^{2+} + \text{EA} \rightarrow [\text{Cu}_2\text{EA}(\text{H}_2\text{O})_8]^{2+} + 8\text{H}_2\text{O} \quad (\Delta S = +\text{ive})$$
$$3[\text{Cu}(\text{H}_2\text{O})_6]^{2+} + 2\text{EA} \rightarrow [\text{Cu}_3(\text{EA})_2(\text{H}_2\text{O})_{10}]^{2+} + 8\text{H}_2\text{O} \quad (\Delta S = +\text{ive})$$
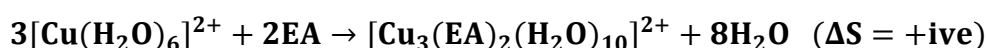
Equation 2: Represents complexation reactions from Figure 8.

The complexation reaction is a spontaneous mechanism as the reaction enthalpy is negative and there is an increase in entropy (due to the loss of multiple aqua ligands in the Hexaaquacopper (II) complex (Figure 2)), which results in an overall negative Gibbs free energy value (as shown by Equation 3). Moreover, the chelate is more stable than the hydrated complex due to the previously mentioned chelate effect (Section 4.3).

$$\Delta G = \Delta H - T\Delta S \text{ [Equation 3]}$$

$\underline{\Delta G}$ = Change in Gibbs free energy | $\underline{\Delta H}$ = Enthalpy | $\underline{T}$ = Temperature | $\underline{\Delta S}$ = Change in entropy

Having understood the modes of interaction, we can now comprehensively investigate the variables of the study in order to optimize and predict the results of the experimentation.

4.8 Effect of Solvent

Before the complexation and chelation processes can begin, ligands must first be extracted from the PPP. The solvent with the highest degree of interaction with the ligands will have the highest extraction efficiency and can lead to high interactive affinity. This is because it can overcome the intermolecular forces keeping the ligands together *(Burke)*. The major factors affecting the interaction are the solvent's polarity and intermolecular forces *(Burke)*.

Figure 9: Solvated clusters of GA. Solvent molecules form hydrogen bonds (dash lines) with the hydroxyl and carboxylic groups of GA, dissolving it. (MolView)
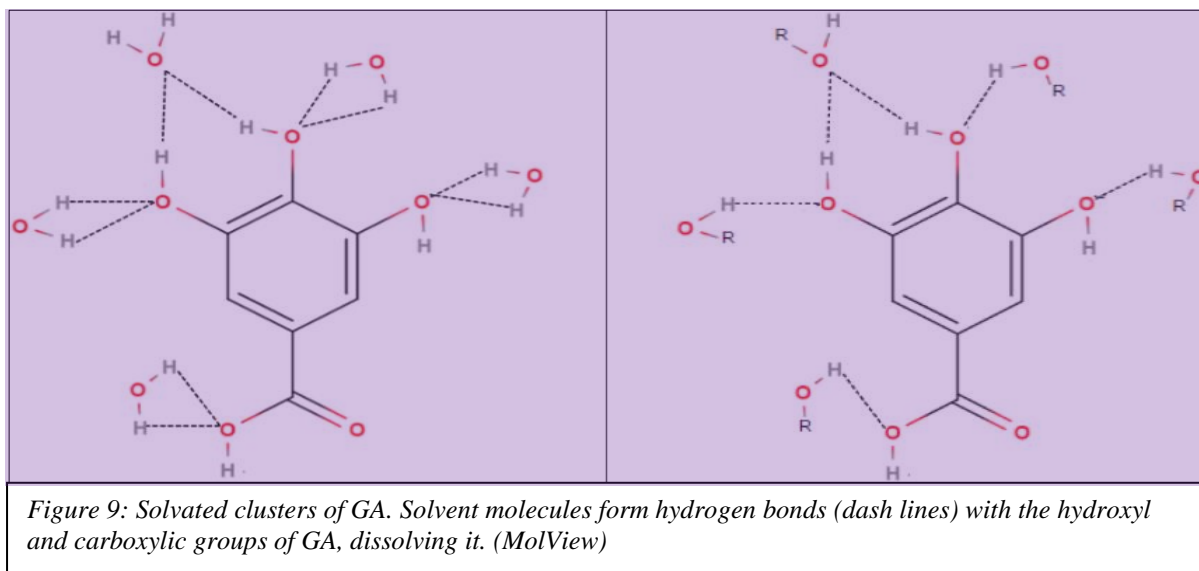
The polarity of the solvent determines its ability to interact with the polar groups of GA, particularly the hydroxyl and carboxylic acid groups as shown in Figure 9. Due to its singular aromatic ring, GA's solvation is more significantly influenced by polar interactions over non-polar interactions. This indicates that the polar water molecules should demonstrate higher solubility for GA than the moderately polar methanol and ethanol molecules as polar solvents would effectively interact with the polar functional groups of GA, thus solvating it.
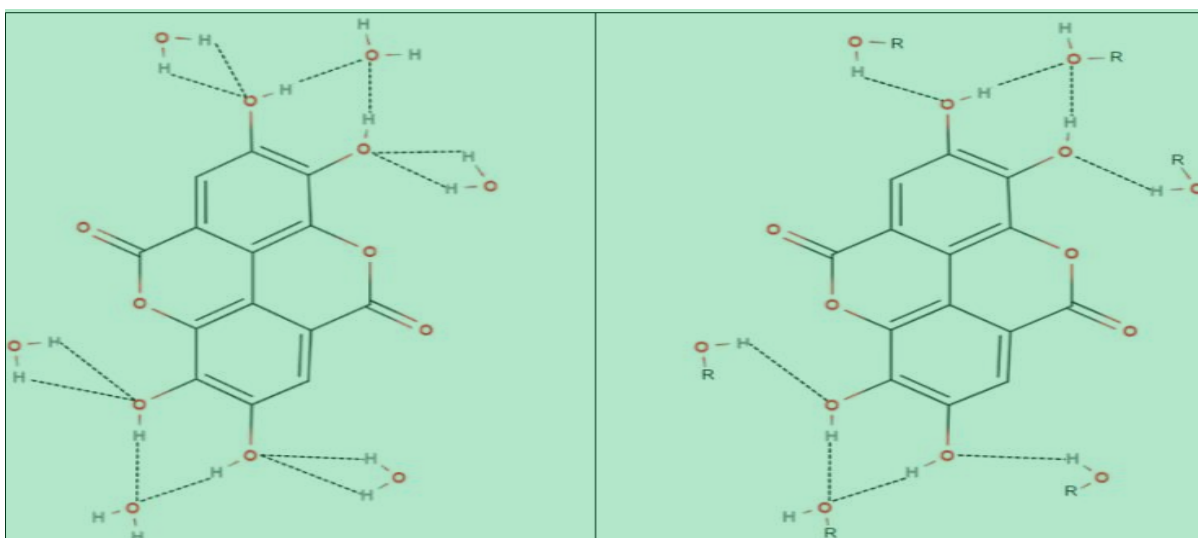
Figure 10: Solvated clusters of EA. Solvent molecules form hydrogen bonds (dash lines) with the hydroxyl groups of EA, dissolving it. (MolView)

On the other hand, EA's solvation is more influenced by van der Waals forces. The heavy condensed aromatic rings in EA seen in Figure 10 should facilitate extensive interactions with large, non-polar molecules through van der Waals forces, due to the higher surface area and electron density of the aromatic groups in EA compared to smaller arenes like GA. While EA has hydroxyl groups capable of hydrogen bonding, its condensed aromatic structure restricts the effectiveness of these interactions, thus making van der Waals forces more prominent in the solvatoin of EA. Hence, methanol and ethanol, with their higher electron density and surface area relative to water, should exhibit enhanced solubility of EA compared to water.

Literature data validates this - GA *(Daneshfar, Ghaziaskar and Homayoun)* **and EA** *(Bala, Bhardwaj and Hariharan)* **are more soluble in methanol and ethanol than water (with ethanol being in the middle for both acids)**. Therefore, taking a lead from the existing literature, the present study evaluates the efficiency of water, methanol, ethanol, and their binary counterparts in extraction of ligands from PPP. This finding will be useful for framing the first hypothesis.

4.9 Effect of pH Environment

Another factor to optimize is the pH of the complexation environment. The pH can significantly affect the complexation efficiency of the PPP extract. This is because pK_a values govern the deprotonation behavior of the molecules. The extent of complexation is strongly influenced by how these molecules deprotonate at different pH levels.

In alkaline conditions, the GA will deprotonate, owing to the presence of a carboxylic and three hydroxyl groups (Figure 5). Its first pK_a (Table 1) corresponds to the carboxylic group which deprotonates first *(Huguenin, Hamady and Bourson)*. The following pK_a values in Table 1 correspond to the hydroxyl groups *(Huguenin, Hamady and Bourson)*.

As the alkalinity of the complexing solution increases from slightly acidic to highly basic, GA will undergo a greater degree of deprotonation, ultimately forming the gallate anion shown in Figure 11. This gradual ionization enhances its ability to act as a ligand since the ions have a greater interactive ability, specifically through the deprotonated carboxyl and hydroxyl groups, hence increasing the EI.

Figure 11: Ionic structures of gallate and ellagate anions. Negative charges marked on the oxygen ions of the deprotonated carboxyl (for GA) and hydroxyl groups. (MolView)
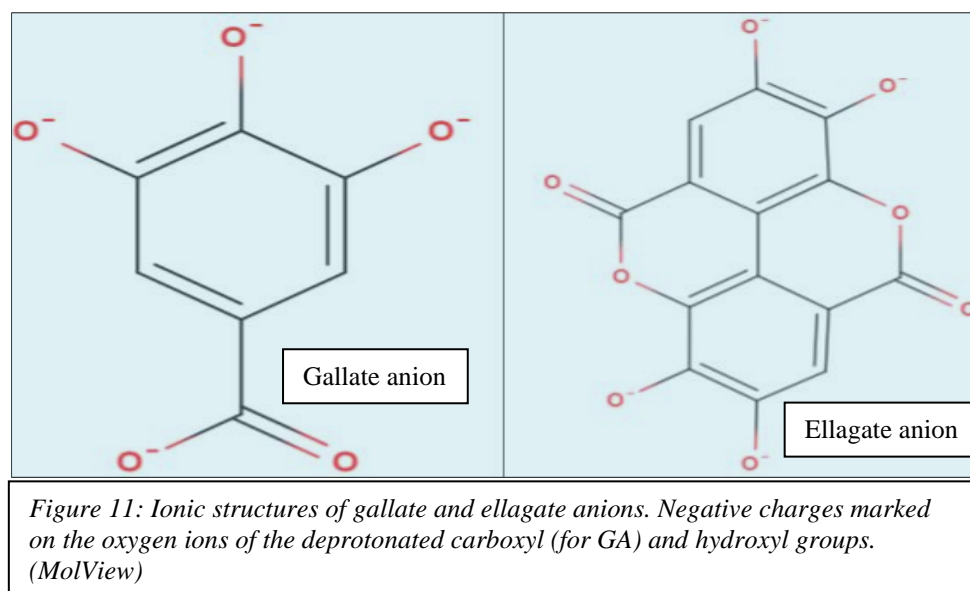
Table 1: pK_a values for GA (Huguenin, Hamady and Bourson) and EA (Muñoz-Muñoz, Gracia-Molina and Garcia-Molina).

17

pK$_a$ for GA	pK$_a$ for EA
4.4 ± 0.1	6.3
8.7 ± 0.1	
10.4 ± 0.1	11.2
11.4 ± 0.1	

EA is peculiar in that it only has two pK$_a$ values (Table 1) for four hydroxyl groups (Figure 5). This arises from the fact that EA is a symmetrical dimer – a molecule consisting of two identical molecules linked together – thus functioning as a dilactone between two GA molecules, with their benzene rings connected by a carbon-carbon bond *(Muñoz-Muñoz, Gracia-Molina and Garcia-Molina)*.

By looking at Table 1, we can determine that EA will have a similar situation as GA since, in neutral and highly alkaline conditions, the pH of the complexing solution would exceed its both its pK$_a$ values, causing all the hydroxyl groups in the molecule to deprotonate and form the ellagate anion (Figure 11), leading to greater complexation between EA and Cu ions.

However, the presence of excess hydroxide ions (OH$^-$) in an alkaline environment could compete with the anions for binding with the Cu ions. **This competition may lead to the formation of insoluble Cu hydroxide precipitates, decreasing the availability of free Cu ions to form complexes with the extracted ligands, thus potentially affecting the EI.**

$$Cu^{2+}_{(aq)} + 2OH^-_{(aq)} \rightarrow Cu(OH)_{2(s)} \downarrow$$
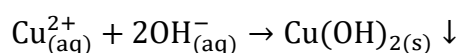
Equation 4: Chemical equation for the possible formation of Cu (II) hydroxide in alkaline environments.

Figure 12: Protonation of the hydroxyl group in low pH environments (MolView)
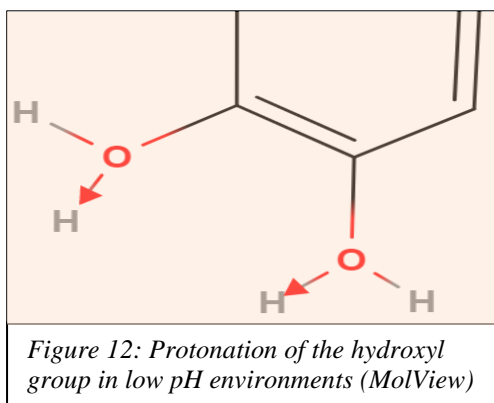
The opposite effect is expected in acidic conditions. The increased protonation of the oxygen ion in the carboxyl (for GA) and hydroxyl groups (due to the formation of a dative bond as shown in Figure 12) present in GA and EA should negatively affect complex formation since the oxygen ions' lone pairs are used for the protonation of the hydroxyl group, reducing number of available binding sites in the ligands. Moreover, the excess H^+ ions in the acidic medium will compete with the already weakened ligands for the Cu ions, further negatively affecting the EI.

4.10 Determination of Extent of Interaction

The most suitable method to determine the efficacy of the experiments is UV-Visible spectroscopy, an analytical technique used for deducing the characteristics of metal-ligand complexes by their photon absorption at varying wavelengths *(Edinburgh Instruments)*. This method hinges on the Beer-Lambert's Law, which correlates the absorbance value from the spectrophotometer with the concentration of metal ions in the solution:

$$A = \varepsilon cl \text{ [Equation 5]}$$

A = Absorbance value | **ε** = Molar absorption | **c** = Concentration | **l** = Path Length

The spectrophotometer displays the amount of light absorbed by the solution in the cuvette. This absorbance value is inversely proportional to the metal-ligand complex concentration in the solution.

The λ_{max} value is the wavelength at which Cu^{2+} exhibits the highest absorbance. After complexation, the absorbance at λ_{max} is determined to calculate complexing efficiency:

$$\text{EI } (\%) = \frac{Am - Ac}{Am} \times 100 \text{ [Equation 6]}$$

> **EI** = Extent of interaction | **Am** = Absorbance of metal ion | **Ac** = Absorbance of complex solution

5 Hypothesis

5.1 Hypothesis 1 – Solvent Performance

As elaborated upon in Section 4.8, literature data suggests that methanol would be the most performant solvent compared to ethanol and water as it strikes a balance between polarity and van Der Waals interactions (relative to ethanol and water), leading to a higher expected complexation.

The diluted counterparts of methanol and ethanol should see a lower EI than the pure solutions since diluting the solvents diminishes their ability to extract non-polar ligands, hence negatively impacting their ligand extraction capability.

> **Methanol > Ethanol > Water > 50% Methanol > 50% Ethanol**

5.2 Hypothesis 2 – Effect of PPP Mass Used

As the mass of the PPP used for extraction increases, the number of interacting species which could be extracted increases as well. As such, there should be a higher extraction yield and thus a higher ligand:Cu^{2+} ratio, leading to higher EI.

> **0.075 > 0.050 > 0.025g**

5.3 Hypothesis 3 – Effect of Metal Ion concentration

A higher concentration of the Cu^{2+} ion will result in more complexation as there will be a greater number of cations per unit volume, thus there will be a greater chance of a successful collision (and complexation) of the ligands and the Cu ions.

$$0.075 > 0.05 > 0.025 \text{ moldm}^{-3}$$

5.4 Hypothesis 4 – Effect of Metal Ligand Voluminal Ratio

The most optimal metal-to-ligand ratio should be around 1:2. This ratio balances the total number of empty orbitals in Cu ions with the total number of binding sites in the ligands.

$$10:20 > 10:30 > 20:30 > 10:10 > 30:20 > 20:10 > 30:10$$

5.5 Hypothesis 5 – Effect of pH Environment

The EI of the PPP extract solution with Cu is expected to be lower in acidic conditions as discussed in Section 4.9. Moreover, it is expected that pH 7 will have a similar EI value as its non-pH mediated part since both should have similar pH conditions during complexation.

$$\text{pH 2} < \text{pH 5} < \text{pH 7} \approx \text{No pH mediation}$$

6 Preliminary Exploration

Preliminary studies were conducted in order to set the fixed variables and to determine a suitable range for the independent variables.

6.1 UV-Vis Spectroscopy

6.1.1 Lambda Max Determination

Graph 1: Graph of absorbance vs. wavelength for CuSO$_{4(aq)}$.
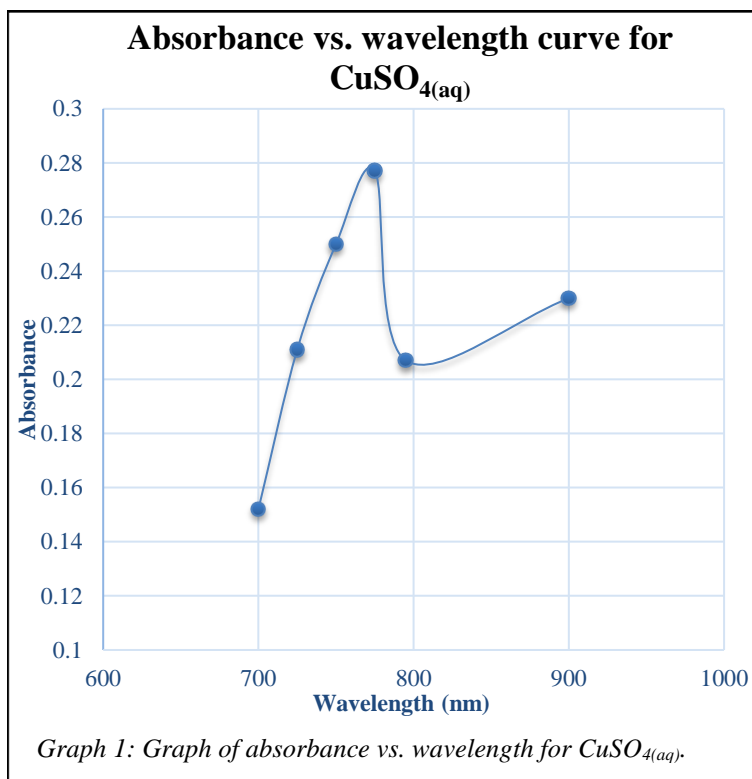
The determination of the λ_{max} value is essential for this study as it will be used to determine the EI. The lambda scan graph for 0.05 moldm^{-3} hydrated copper (II) sulfate (CuSO$_4$.xH$_2$O) solution (Graph 2) has a peak at 775 nm which was set as the λ_{max} value.

6.1.2 Standard Calibration Curve

Graph 2: Standard curve of CuSO$_{4(aq)}$ at λ_{max} (775 nm)
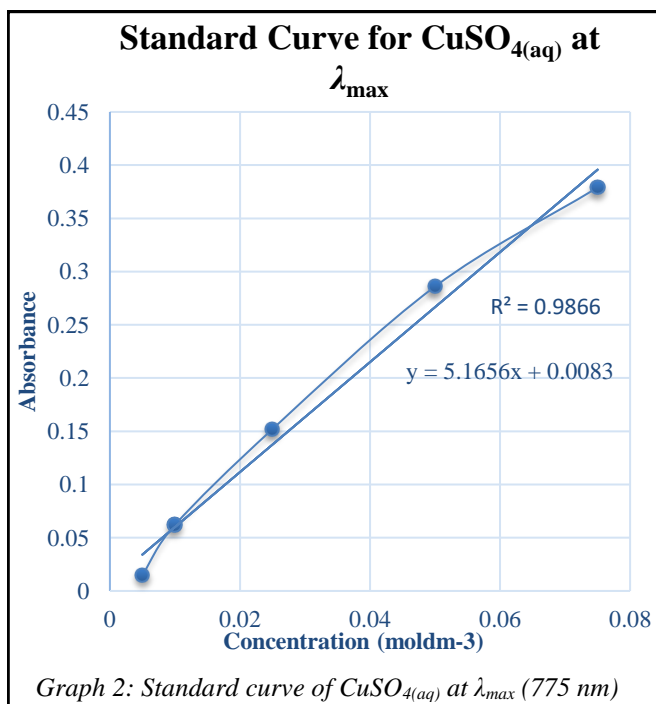
A calibration curve is used to plot the linear relationship between the absorbance and concentration of CuSO$_4$ standard according to Beer-Lambert's Law. The λ_{max} wavelength is used to measure the absorbance at each concentration. The high R^2 value proves the precision and reliability of the spectrophotometer used.

6.2 Selection of Extraction Method

Various extraction methods were tested – shaking, heating, and heated magnetic stirring –to determine which would yield the highest degree of interaction. The results of this investigation are shown in Flowchart 2 below.

Flowchart 2: Process flowchart for the selection of the ligand extraction method. (Lucidchart)
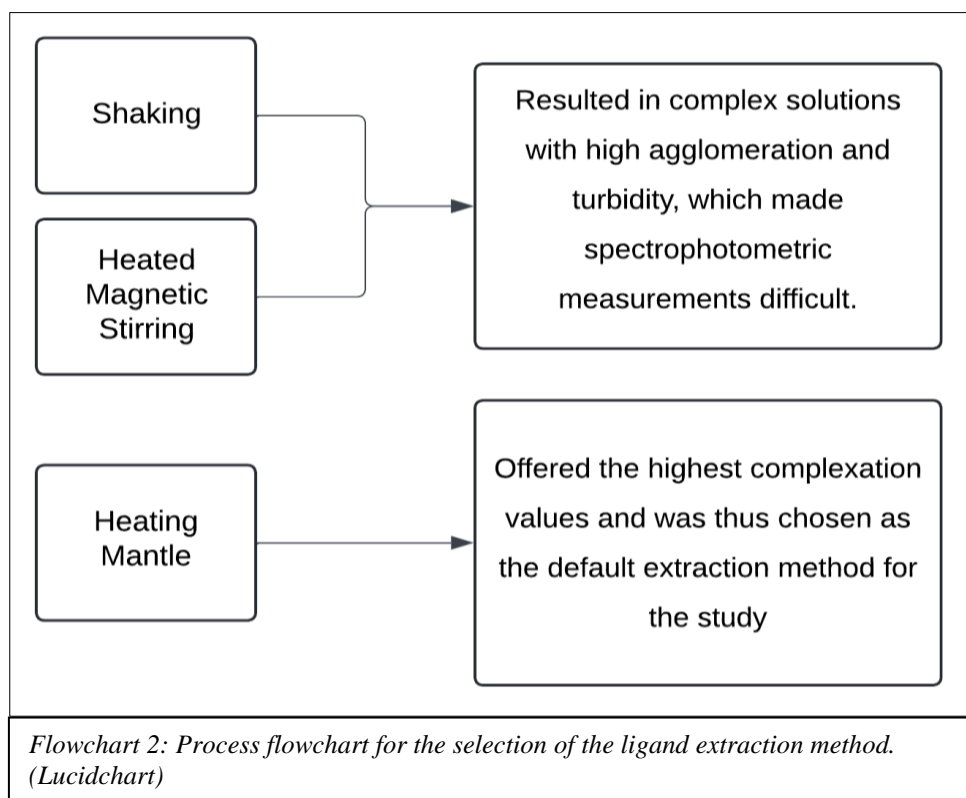
6.3 Selection of Boiling Duration

A range of boiling durations were chosen – 5, 10, and 15 minutes – to determine how thermal degradation and solvent solubility affect the metal interaction efficiency of the solutions. **Finally, 5 minutes was selected since the ethanol solutions experienced significant evaporation and were boiling off during the 10 and 15-minute durations.**

6.4 Selection of PPP Mass

0.100, 0.075, 0.050 and 0.025 grams of PPP were used in the preliminary tests to determine the extent of extraction of ligands. **0.100g was not used for the actual study because the**

complexed solutions were too turbid to make reliable spectrophotometric

measurements.

7 Variables

7.1 Independent

Table 2: Independent variables of the study.	
Solvents	Water, Ethanol, Methanol, 50% Ethanol, 50% Methanol
Mass of PPP (g)	0.025, 0.050, 0.075
Concentration of Cu^{2+} ($moldm^{-3}$)	0.025, 0.050, 0.075
Solution:Cu^{2+} Voluminal Ratio (cm^3)	10:20, 10:30, 20:30, 10:10, 30:20, 20:10, 30:10
pH for complex solutions	2, 5, 7

7.2 Dependent

Table 3: Dependent variables of the study.
Absorbance value for each solution at λ_{max}
Calculated value of EI from the absorbance (using Equation 6)

7.3 Control

Table 4: Control variables of the study.		
Variable	**Value**	**Justification**
Volume of Solvent Used (cm^3)	50 ± 0.5	Ensures that a consistent amount of ligands are extracted from the PPP by each solvent through the experiments. Volume measured using a $100 \pm 0.1cm^3$ graduated cylinder for each experiment.

Boiling Duration (minutes)	5 ± 0.5	Also used to ensure a consistent degree of ligand extraction across all experiments. A timer was used to monitor the boiling duration for each sample.
Complexation Period (hours)	3	Samples were left undisturbed in a rotary shaker to complex for 3 hours. This allows sufficient time for the complexation reaction to reach equilibrium, making sure that the Cu ions are maximally complexed.
Temperature (°C)	28 ± 1	Minimizes changes in reaction kinetics and mechanisms to reduce irregularities. Experiments were conducted in the temperature-controlled lab environment.

8 Preparation of Reagents

Table 5: Preparation procedure for CuSO₄ standards.

8.1 Preparation of CuSO$_4$ standards of varying concentrations	
CuSO$_4$ Concentration in (moldm^{-3})	**Mass required for 100cm^3 of standard (g)**
0.025	0.624 ± 0.001
0.050	1.248 ± 0.001
0.075	1.872 ± 0.001

The required mass of CuSO$_4$ (M_r = 249.609) for each concentration was measured using an electronic top pan balance and diluted to 100.0 ± 0.5cm^3 using a standard flask. Before use, the standard flasks were shaken thoroughly to ensure uniform composition.

Table 6: Preparation procedure for ligand solutions.

8.2 Preparation of ligand solutions

Step 1: The 0.025g of PPP (as measured by the electronic top pan balance) is transferred to a beaker using a spatula.

Step 2: Measured using a 100cm^3 measuring cylinder, 50cm^3 of the solvent is transferred to the beaker.

Step 3: The beaker is then placed in the heating mantle for the required duration at 100°C.

Step 4: After a minute long cooldown period, the ligand solution is filtered to remove the undissolved PPP.

Table 7: Preparation procedure for pH buffer solutions.

8.3 Preparation of Buffer Solutions		
pH 2 Buffer	**pH 5 Buffer**	**pH 7 Buffer**
Step 1: Using a measuring cylinder, 13.0±0.5 cm^3 of 0.2 moldm^{-3} of hydrochloric acid (prepared as per Section 17.2.1), was measured and transferred to a 250cm^3 beaker.	**Step 1:** Using a measuring cylinder, 59.0±0.5 cm^3 of Glacial acetic acid (prepared as per Section 17.2.2), was measured and transferred to a 250cm^3 beaker.	**Step 1:** Using a measuring cylinder, 100±0.5 cm^3 of distilled water was measured and transferred to a 100cm^3 beaker.
Step 2: Using a measuring cylinder, 50±0.5 cm^3 of 0.2 moldm^{-3} of potassium chloride (prepared as per Section 17.2.1), was measured and transferred to the same 250cm^3 beaker containing hydrochloric acid.	**Step 2:** Using a measuring cylinder, 141±0.5 cm^3 of Sodium acetate trihydrate (prepared as per Section 17.2.2), was measured and transferred to the same 250cm^3 beaker containing glacial acetic acid to obtain pH 5 buffer solution.	**Step 2:** The contents of a pH 7 buffer preparation capsule was added to the beaker and the solution was stirred thoroughly to obtain pH 7 buffer solution.
Step 3: Using a measuring cylinder, 137±0.5 cm^3 of distilled water was measured and transferred to the aforementioned 250cm^3 beaker to obtain pH 2 buffer solution.		

9 Methodology

Table 8: Preparation procedure for complex solutions.
9.1 Preparation of complex solutions
Step 1: Using a pipette, the required volume of the ligand solution (as per the metal:ligand ratio) is transferred to a flask.   **Step 2:** The required volume and concentration of the $CuSO_4$ standard is added to the flask using a pipette.   **Step 3:** The flask is then left to equilibrate in the rotary shaker for 3 hours.   **Step 4:** Then a sample is taken from the complexed solution in the flask for further analysis.

Table 9: Preparation procedure for complex solutions with pH buffer.
9.2 Preparation of complex solutions with buffer
Step 1: The required volume of the ligand solution is transferred to a flask using a pipette.   **Step 2:** $5cm^3$ of the required buffer is added to the ligand solution using a pipette.   **Step 3:** The required volume and concentration of the Cu standard is added to the flask using a pipette.   **Step 4:** The flask is then left to equilibrate in the rotary shaker for 3 hours.   **Step 5:** Then a sample is taken from the complexed solution in the flask for further analysis.

10 Data Collection

The calculations for the uncertainties of the varying concentrations of metal ion solutions are given in the Appendix (Section 17.1).

10.1 Qualitative Data

Table 10: Qualitative data for the complexed solutions for varying solvents.

10.1.1 Complex Solutions for Varying Solvents	
Solvent	**Observation**
Water	Olive green, slight brown precipitates
Ethanol	Olive green
Methanol	Olive green
50% Ethanol	Olive green
50% Methanol	Pale light blue

Table 11: Qualitative data for the complexed solutions for varying PPP mass (g).

10.1.2 Complex Solutions at Varying PPP Mass (± 0.001) (g)			
Solvent/PPP Mass (in grams)	**0.025**	**0.050**	**0.075**
Water	Olive green, brown precipitates	Olive green, slight brown precipitates	Olive green
Ethanol	Olive green	Olive green	Olive green
Methanol	Pale light blue	Olive green	Olive green

Table 12: Qualitative data for the complexed solutions for varying Cu concentration (moldm^{-3}).

10.1.3 Complex Solutions at Varying Cu Concentrations (moldm^{-3})			
Solvent/Concentration	**0.025 ± 1.65×10^{-4}**	**0.050 ± 1.45×10^{-4}**	**0.075 ± 1.38×10^{-4}**
Water	Pale olive green	Olive green, slight brown precipitates	Olive green, brown precipitates
Ethanol	Pale olive green	Olive green	Olive green
Methanol	Pale olive green	Olive green	Olive green

Table 13: Qualitative data for the complexed solutions for varying voluminal ratios (cm^3).

10.1.4 Complex Solutions for Varying Cu^{2+}:Ligand Voluminal Ratios (cm^3)		
Water	**10:10**	Olive green, slight brown precipitates
	10:20	Pale teal
	10:30	Olive green
	20:10	Pale light blue, brown precipitates
	20:30	Pale olive green
	30:10	Olive green, brown precipitates
	30:20	Olive green, slight brown precipitation
Methanol	**10:10**	Golden yellow
	10:20	Olive green
	10:30	Olive green
	20:10	Olive green
	20:30	Pale olive green
	30:10	Teal
	30:20	Olive green

Table 14: Qualitative data for the complexed solutions for varying pH and PPP mass (g) at 0.075 $moldm^{-3}$ Cu concentration.

10.1.5 Complex Solutions at Varying pH and PPP Mass ($\pm$ 0.001) (g) (0.075 $moldm^{-3}$ Cu^{2+})			
pH/PPP Mass (in grams)	**0.025**	**0.050**	**0.075**
2	Olive green	Pale teal	Olive green
5	Olive green	Olive green	Olive green
7	Olive green	Pale teal	Olive green

10.2 Quantitative Data – Absorbance Values

Table 15: Quantitative data for the complexed solutions for varying solvents.	
10.2.1 Complex Solutions for Varying Solvents	
Solvent	**Absorbance**
Water	0.136
Ethanol	0.139
Methanol	0.105
50% Ethanol	0.233
50% Methanol	0.210

Table 16: Quantitative data for the complexed solutions for varying PPP mass (g).			
10.2.2 Complex Solutions at Varying PPP Mass ($\pm$ 0.001) (g)			
Solvent/PPP Mass (in grams)	**0.025**	**0.050**	**0.075**
Water	0.177	0.136	0.122
Ethanol	0.194	0.139	0.116
Methanol	0.150	0.105	0.083

Table 17: Quantitative data for the complexed solutions for varying Cu concentration ($moldm^{-3}$).			
10.2.3 Complex Solutions at Varying Cu Concentrations ($moldm^{-3}$)			
Solvent/Concentration	**0.025 $\pm$ 1.65$\times10^{-4}$**	**0.050 $\pm$ 1.45$\times10^{-4}$**	**0.075 $\pm$ 1.38$\times10^{-4}$**
Water	0.116	0.136	0.183
Ethanol	0.119	0.139	0.186
Methanol	0.069	0.105	0.158

Table 18: Quantitative data for the complexed solutions for varying voluminal ratios (cm³).

10.2.4 Complex Solutions for Varying Cu²⁺:Ligand Voluminal Ratios (cm³)		
Water	**10:10**	0.208
	10:20	0.122
	10:30	0.213
	20:10	0.202
	20:30	0.188
	30:10	0.211
	30:20	0.208
Methanol	**10:10**	0.177
	10:20	0.061
	10:30	0.180
	20:10	0.188
	20:30	0.158
	30:10	0.183
	30:20	0.183

Table 19: Quantitative data for the complexed solutions for varying pH and PPP mass (g) at 0.075 moldm⁻³ Cu concentration.

10.2.5 Complex Solutions at Varying pH and PPP Mass (± 0.001) (g) (0.075 moldm⁻³ Cu²⁺)			
pH/PPP Mass (in grams)	**0.025**	**0.050**	**0.075**
2	0.202	0.177	0.155
5	0.183	0.249	0.139
7	0.166	0.139	0.125

Table 20: Quantitative data for the complexed solutions for varying pH and PPP mass (g) at 0.075 moldm^{-3} Cu concentration.

10.2.6 Complex Solutions at Varying pH and PPP Mass ($\pm$ 0.001) (g) (0.075 moldm^{-3} Cu^{2+})			
pH/PPP Mass (in grams)	**0.025**	**0.050**	**0.075**
2	0.208	0.205	0.169
5	0.183	0.169	0.141
7	0.147	0.139	0.130

11 Data Processing – EI%

Sample Data Processing (for EI%)				
Solvent	**PPP Mass (g)**	**Cu standard concentration (moldm^{-3})**	**Absorbance of complex solution at 775 nm (A$_c$)**	**Absorbance of 0.05 moldm^{-3} at 775 nm (A$_m$)**
Water	0.01 $\pm$ 0.001	0.050 $\pm$ 1.45$\times$10^{-4}	0.177	0.277
(Equation 6) **Extent of Interaction (%)** $= \frac{Am - Ac}{Am} \times 100 = \frac{0.277 - 0.177}{0.177} \times 100 = \textbf{36\%}$				

Table 21: EI% data for the complexed solutions for varying solvents.

11.1 Complex Solutions for Varying Solvents	
Solvent	**EI%**
Water	51%
Ethanol	50%
Methanol	62%
50% Ethanol	16%
50% Methanol	24%

Table 22: EI% data for the complexed solutions for varying PPP mass (g).

11.2 Complex Solutions at Varying PPP Mass (± 0.001) (g)			
Solvent/PPP Mass (in grams)	**0.025**	**0.050**	**0.075**
Water	36%	51%	56%
Ethanol	30%	50%	58%
Methanol	46%	62%	70%

Table 23: EI% data for the complexed solutions for varying Cu concentration (moldm^{-3}).

11.3 Complex Solutions at Varying Cu Concentrations (moldm^{-3})			
Solvent/Concentration	**0.025 ± 1.65×10^{-4}**	**0.050 ± 1.45×10^{-4}**	**0.075 ± 1.38×10^{-4}**
Water	58%	51%	34%
Ethanol	57%	50%	33%
Methanol	75%	62%	43%

Table 24: EI% data for the complexed solutions for varying voluminal ratios (cm^3).

11.4 Complex Solutions for Varying Cu^{2+}:Ligand Voluminal Ratios (cm^3)		
Water	**10:10**	25%
	10:20	56%
	10:30	23%
	20:10	27%
	20:30	32%
	30:10	24%
	30:20	25%
Methanol	**10:10**	36%
	10:20	78%

	10:30	35%
	20:10	32%
	20:30	43%
	30:10	34%
	30:20	34%

Table 25: EI% data for the complexed solutions for varying pH and PPP mass (g) at 0.075 moldm^{-3} Cu concentration.

11.5 Complex Solutions at Varying pH and PPP Mass (± 0.001) (g) (0.075 moldm^{-3} Cu^{2+})

pH/PPP Mass (in grams)	0.025	0.050	0.075
2	27%	34%	40%
5	36%	10%	50%
7	44%	50%	55%

12 Analysis

12.1 Analysis 1 – Solvent Performance

Graph 3: EI of various solvents (0.05g PPP: 0.05moldm^3 Cu^{2+}: 10:20)
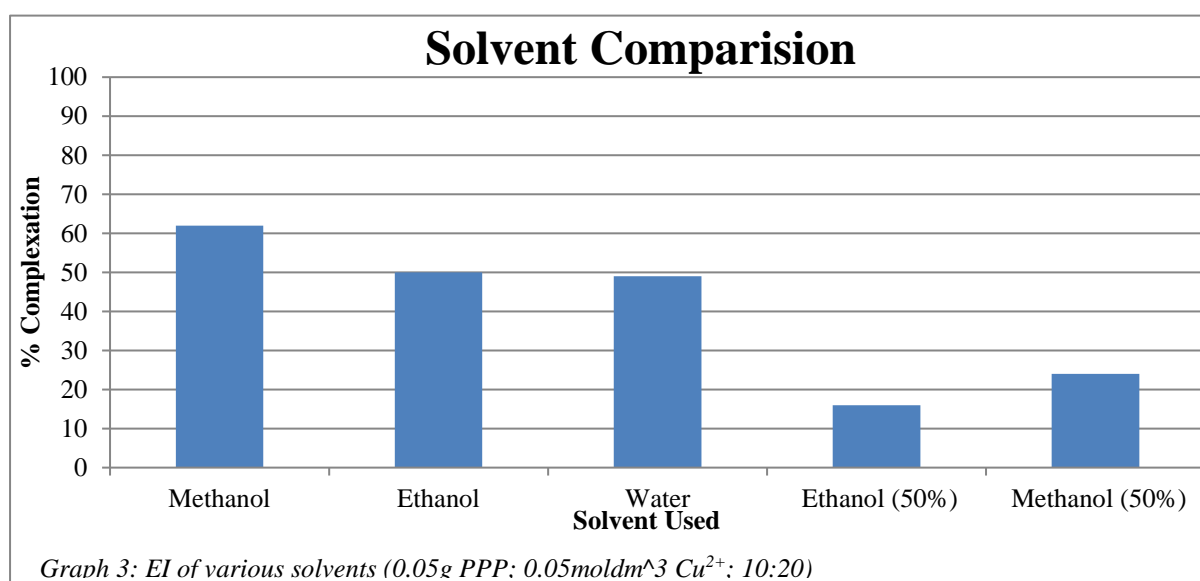
Graph 3 shows the EI of various solvents under the same extraction and complexation conditions. The first trend to note is the fall in EI from methanol to ethanol/water (~12%). The next trend is the fall in the EI from methanol to 50% methanol (38%) and ethanol to 50% ethanol (34%). **These values mostly corroborate Hypothesis 1 – methanol is by far the most performant solvent (as it balances van der Waal forces and polarity), while diluted ethanol is the least performant.** These trends concretize methanol's superior ligand extraction abilities compared to ethanol and water. Given that the function of the polyphenolic derivates from PP as chelators is now established, it is reasonable to delve deeper into the specificities of these chelate-metal ion interactions – first, however, this requires an understanding of the polyphenolic profile of PPs.

Water's EI is comparable to that of ethanol (Graph 3). This deviation from the hypothesized trend is not justified by the expected interactions between the water molecules, GA, and EA (Section 4.8). Hence, water's unexpectedly high EI could be explained by the extraction of other highly polar ligands from PPP that complex with the Cu ions. Since, as mentioned in

Section 4.5, non-GA and EA polyphenols such as catechin and epicatechin (Figure 6) make up 20-40% of the peel (Figure 4). Moreover, as explained in literature *(Kaderides, Goula and Adamopoulos)*, water molecules have a smaller size than GA and EA, **which may enable them to penetrate the cell walls of the PPP to a greater extent than the other, larger solvent molecules and thus dissolve the ligands present within, leading to a higher-than-expected extraction efficiency and thus higher EI values.** The literature references used in Section 4.8 used commercially-available GA and EA which were not extracted through any cell matrices – this was not accounted for in the framing of Hypothesis 1, most likely leading to water's unpredicted EI value.

12.2 Analysis 2 – Effect of PPP Mass Used

Graph 4: EI of various PPP masses (0.05moldm^3 Cu^{2+}; 10:20)
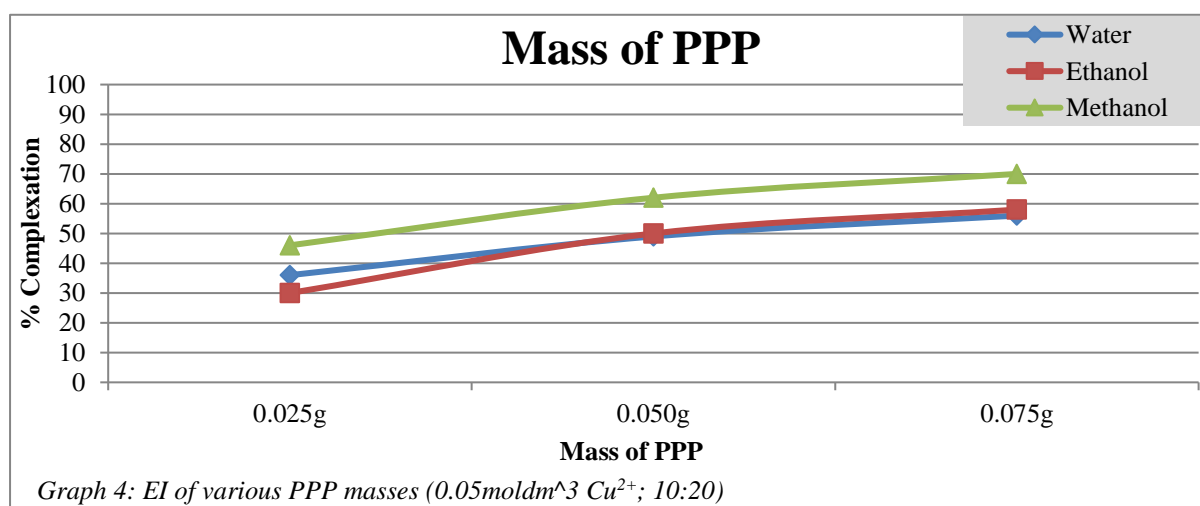
Graph 4 shows the EI of using varying PPP mass for different solvents under the same extraction and complexation conditions. Water and ethanol perform about 12% lower than methanol (Section 12.1), but they are still used for this and most of the preceding tests due to a limitation that methanol faces regarding the aim of the study (Section 14.2). Returning to the graph, it can be observed that EI increases with PPP mass for all solvents. **These values align with the predicted trend in Hypothesis 2.** At 0.050g, water and ethanol have an

equivalent EI (1% difference), and the same applies for 0.075g (2% difference) (while methanol has a higher EI than the other solvents throughout all masses).

The observed plateau of all three lines in the graph as the PPP mass increases could be attributed to the solubility limits of the solvents. As the extraction process progresses and more ligands are dissolved in the solvent, the solution tends to approach its maximum solubility limit. At this point where the solution would have approached its solubility limit, the extent of dissolution diminishes and thus the extraction efficiency at higher masses plateaus as well. This can lead to the plateauing effect in the interacting behavior. The extent of the plateauing will vary based on the specific solubility limit of each solvent – which depends on various factors such as the polarity of the solvent and solute *(Tran and Liu)*. The plateauing effect is displayed numerically in Table 26, wherein the last column demonstrates how the increase in EI is more substantial at lower two masses compared to the higher two masses for all solvents.

Solvent	Increase in EI between 0.025g and 0.050g	Increase in EI between 0.050g and 0.075g	Difference in the increase of the EI
Methanol	16%	8%	-8%
Water	13%	9%	-4%
Ethanol	20%	8%	-12%

Table 26: The percentage change in the EI values for each solvent as the PPP mass increases.

12.3 Analysis 3 – Effect of Metal Ion concentration

Graph 5: EI of various metal ion concentrations (0.075g PPP; 10:20)
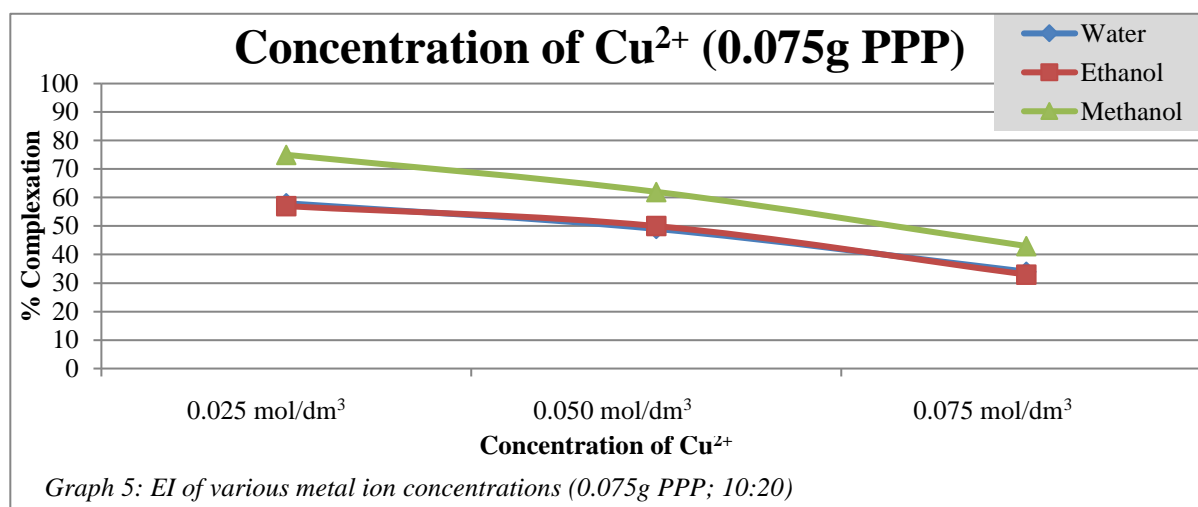
Graph 5 shows the EI of using differing Cu concentrations for different solvents and masses at the same extraction and complexation conditions. It can be observed that the EI falls with increasing Cu concentration, **which goes against the expected trend that was hypothesized in Hypothesis 3.**

A plausible explanation for this comes from the qualitative observations of the experiment's complexed solutions. The occurrence of brown precipitate in the 0.075 moldm^{-3} solutions as well as some of the 0.050 moldm^{-3} solutions (Section 10.1.3) suggests that Cu precipitation occurs at high concentrations, which negatively affects the measured EI. This precipitate may have formed due to the ligands not being able to complex with most of the Cu ions (due to its high availability in higher concentrations), resulting in excess Cu ions settling as precipitate. **The reasoning behind the formation of the precipitate could be attributed to the formation of copper (I) oxide (Cu_2O) in the solution since polyphenols are known to reduce Cu^{2+} to Cu^+ (Section 4.6).**

Solvent	Decrease in EI between	Decrease in EI between	Difference in the decrease of the EI

Table 27: The percentage change in the EI values for each solvent as the Cu concentration increases.

	0.025moldm^{-3} and 0.050moldm^{-3}	0.050moldm^{-3} and 0.075moldm^{-3}	
Methanol	13%	19%	6%
Ethanol	7%	13%	6%
Water	9%	15%	6%

Another observation is that the solvents' performances have a larger drop at 0.075 moldm^{-3} from 0.05moldm^{-3} relative to at 0.050moldm^{-3} from 0.025moldm^{-3} (as shown numerically in the last column of Table 27). This indicates that the **Cu ion saturation concentration for all three solvents is between 0.050 moldm^{-3} and 0.075 moldm^{-3} – after which, the aforementioned precipitation is expected to occur**. Water and ethanol have near identical EI values across the concentrations while methanol is roughly on average 15% more performant than the other two solvents (Graph 5) – which agrees with the difference in solvent performances from Section 12.1.

12.4 Analysis 4 – Effect of Metal Ligand Voluminal Ratio

Graph 6: EI of various voluminal ratios (0.025g PPP; 0.075moldm^3)
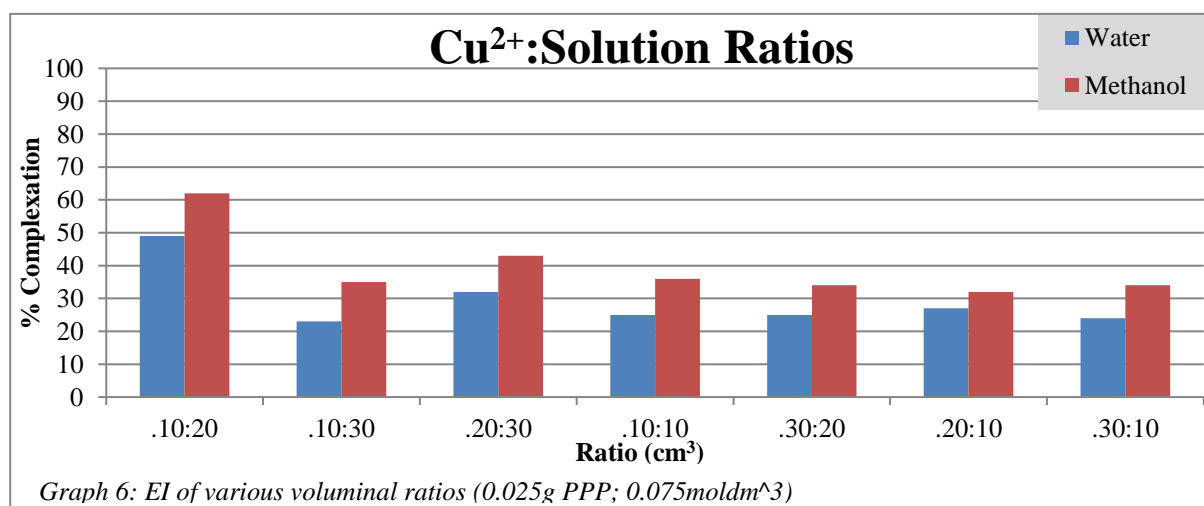
Graph 6 shows the EI of complexed solutions of varying Cu ion-to-ligand solution ratios for methanol and water solvents at the same extraction and complexation conditions. This graph indicates that, aside from the 10:20 and 20:30 ratios, all the ratios for the solvents have

somewhat comparable EI performance (with the maximum difference in EI values for the other ratios being within 10%). This partially contradicts with Hypothesis 4 which predicted that ratios with a lower proportion of metal ions would yield a greater EI value and vice versa.

A possible justification for the lower-than-expected readings for the 10:30 ratio for the solvents could be **steric interference since having a very high ratio of ligands in a solution relative to Cu ions would make it more difficult for complexation to occur through spatial constraints around Cu ions.** The slight bump in EI at the 20:30 ratio for methanol and water (8% and 9% from the preceding ratio for each solvent respectively) indicates that there is a relatively better balance at the 20:30 ratio compared to its following ratios.

The low EI for the 10:10. 30:20, 20:10, and 30:10 ratios can be explained through the formation of Cu precipitate at those ratios (Section 10.1.4) due to excess Cu being present in the complexing solutions.

12.5 Analysis 5 – Effect of pH Environment

Graph 7: EI of various pH and mass combinations (Methanol solvent; 0.025moldm^3 Cu^{2+}; 10:20:10 – metal:ligand:pH buffer)
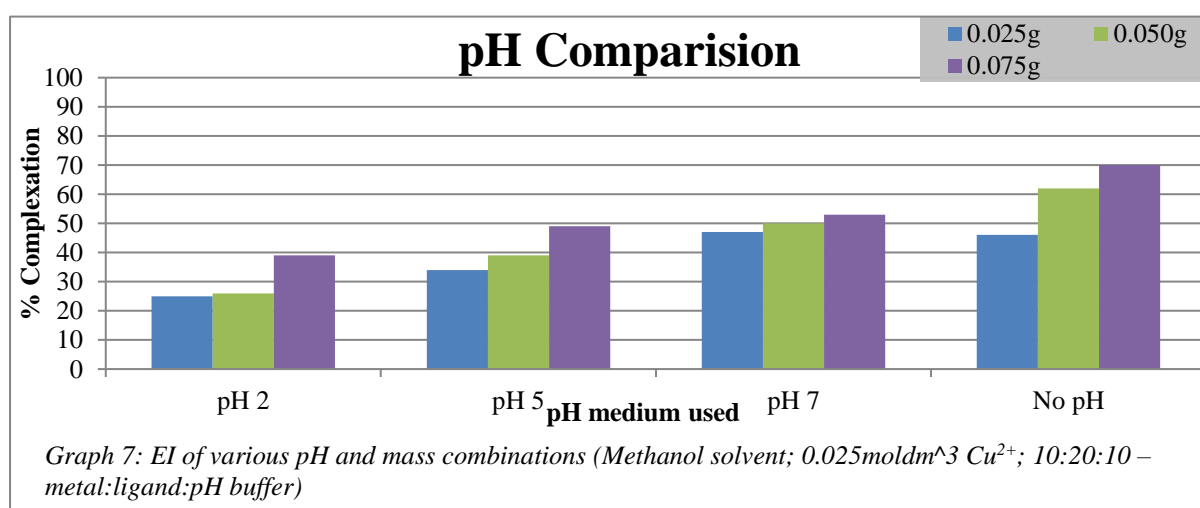
Graph 7 shows the EI of complexed solutions of varying pH and PPP mass at the same extraction and complexation conditions. There is a trend in the graph as seen in the tendency of the EI to rise as the pH goes from acidic to neutral. The readings mostly agree with Hypothesis 5 since a deterioration in the EI is seen with increasing acidity—a trend explored in Section 4.9. However, the extent of complexation in the non-pH mediated environment is generally higher than at pH 7, which does not align with the hypothesis.

In the non-pH mediated experiments, the extent of complexation is higher than in the pH 7 studies for the 0.050 and 0.075g of PPP (by 12% and 17% respectively) while the values for 0.025g PPP are statistically equivalent (1% difference). This could be due to the non-pH mediated complex solutions inheriting an intrinsic alkalinity at a certain point during the complexation mechanism, leading to a greater extent of chelation as covered in Section 4.9.

Since the investigation utilized acidic pH buffers of low alkalinity, the ligands should have undergone partial (at pH 5 and 7) or no deprotonation (pH 2). This means that the completely ionized structures in Figure 11 would not have been formed. Hence, plausible complex structures which may have formed in the pHs used are shown in Figure 13 below.

Figure 13: Plausible complexes that may form in pH 5 and 7. (MolView)
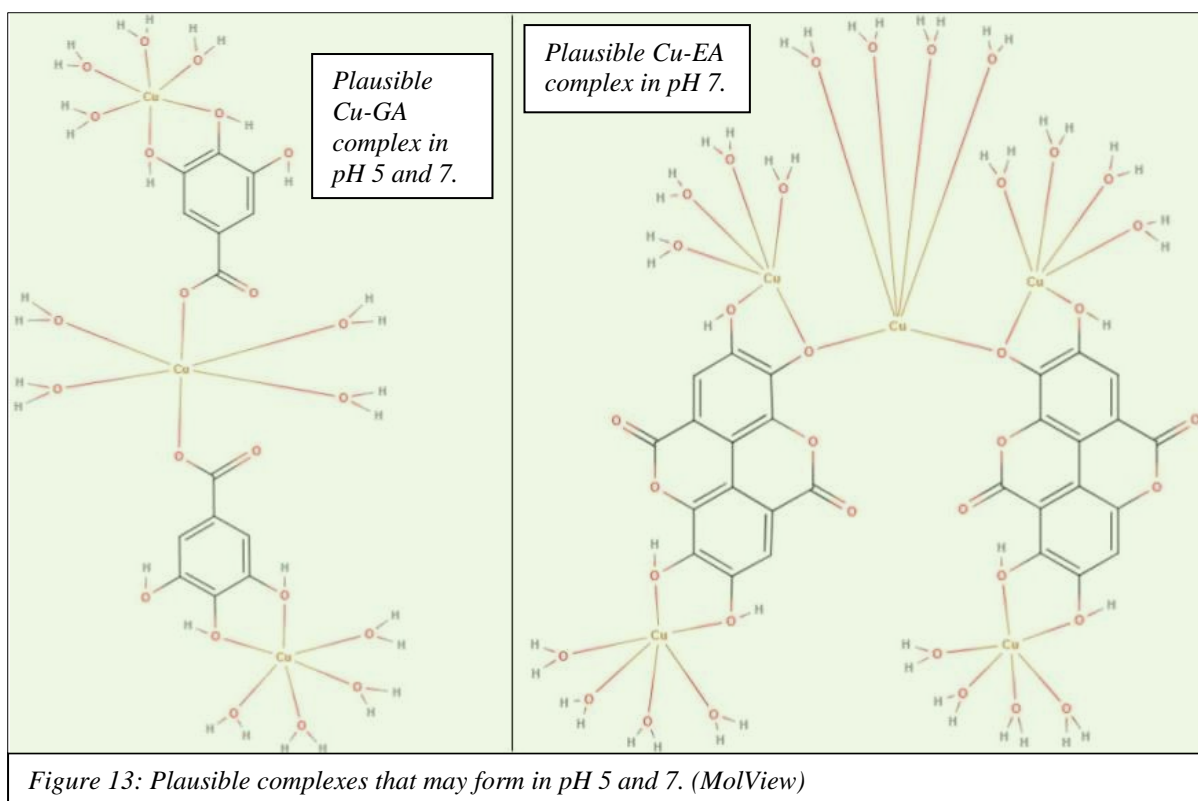
13 Conclusion

The investigation elucidates the potent chelating ability of phenolic acid derivatives, specifically GA and EA, extracted from PPP in complexing with Cu^{2+} ions.

The research explored various parameters to optimize the EI, including the solvent used for extraction, the mass of PPP, the concentration of Cu^{2+} ions, the metal ion-to-ligand ratio, and the pH environment:

- **Methanol has found to be the most effective solvent.**

- **Increasing the PPP mass corresponded with higher EI values.**

- **Unexpectedly, higher concentrations of Cu ions led to a decrease in the measured EI.**

- **The optimal metal-to-ligand ratio was identified as 1:2.**

- **The study also found that a neutral pH condition provided the most favorable environment for complex formation.**

The findings thus illuminate a pathway for fostering a 'green chemistry' approach to water remediation through the use of PPs, which are a readily available and low-cost organic waste product. **Through setting boundaries for optimizing the maximal EI, this study presents a sustainable, waste-to-wealth alternative to traditional synthetic chelating agents for the water treatment processes.**

14 Evaluation

Table 28: Strengths and limitations of the study.	
14.1 Strengths	**14.2 Limitations**
- The study leverages organic waste products (PPs) for water remediation; hence the side-effects of synthetic alternatives such as EDTA are avoided (Section 2). - Granulation of PPs results in an increase in its surface area - this technique being chosen in order to maximize the efficiency of ligand extraction and allow for greater penetration of the plant matrix. - The study establishes PPP as a reservoir of GA and EA which are	- The study establishes methanol as the most performant solvent for the extraction of ligands from PPs (Section 12.1), thus making it an efficient and economical solution for heavy-metal contaminated water treatment in industrial settings. However, its association with volatility *(Medina)* raises concerns about potential detrimental effects, complicating its usage in the long-term. - A larger pH range inclusive of alkaline environments were not tested

possible remediating agents (Section 4.5).	– although a higher EI was expected in those ranges (Section 4.9) – due to the high expected levels of Cu precipitation (Section 4.9) which would have negatively affected the measured EI.
• Using a UV-Visible spectrophotometer ensures a high degree of reliability in the measurements of the degree of interaction between the metal and ligand solution.	• Real-world Cu contaminated water samples were not utilized in this study, potentially indicating that the observed results could differ in real-world scenarios.
• The utilization of a spectrum of readily available organic solvents ensures low economic costs while achieving a high EI.	
• Through exploring a wide array of complexation conditions, the study has effectively asserted PPP as an effective and viable green alternative for the treatment of Cu^{2+} ions in water.	
• The analyses were substantiated with sound reasoning, even in instances where the data did not align with the hypotheses.	

Table 29: Weaknesses of study.

14.3 Weaknesses	
Systematic Errors	Random Errors
• The ligand extraction solution may have contained competing polyphenols which could not be eliminated, possibly hindering the expected results.	• The analytes were prepared only once, potentially affecting the overall reliability of the results. Repeating the tests would enhance the reliability and robustness of the findings.

15 Further Scope

The study can be extended to investigate PPP's efficacy in scavenging additional heavy-metal contaminants such as nickel and zinc, which are also present in heavy-metal polluted water *(Mokarram, Saber and Sheykhi)*. Moreover, further studies could incorporate various breeds of pomegranates (including white pomegranate) to determine how differences in their chemical composition and properties affect the degree of interaction with metal ions. The influence of pre-processing steps on the PPs – for instance, sun-drying and freeze-drying – prior to their granulation could be evaluated to determine the potential effects of these processing methods on their polyphenolic properties and, by extension, their chelating performance.

16 References

1. Akagawa, Mitsugu and Kyozo Suyama. "Amine oxidase-like activity of polyphenols: Mechanism and properties." *European Journal of Biochemistry* 268.7 (2008): 1960. 12 December 2023. <https://febs.onlinelibrary.wiley.com/doi/pdf/10.1046/j.1432-1327.2001.02068.x>.

2. Bala, I., et al. "Analytical methods for assay of ellagic acid and its solubility studies." *Journal of Pharmaceutical and Biomedical Analysis* 40.1 (2006): 209. 23 December 2023.

3. Barret, Jack. *Inorganic chemistry in aqueous solution*. Vol. 21. London: Royal Society of Chemistry, 2003. 20 December 2023. <https://books.rsc.org/books/monograph/307/Inorganic-Chemistry-in-Aqueous-Solution>.

4. Belščak-Cvitanović, Ana, et al. "Overview of polyphenols and their properties." *Polyphenols: Properties, Recovery, and Applications* (2018): 3, 12, 16-18. 30 November 2023.

5. Brown, Catrin and Mike Ford. *Higher Level Chemistry 2nd Edition*. 2. Harlow: Pearson Baccalaureate, 2014. Book. 14 November 2023.

6. Burke, John. "Part 1 - Solutions and Molecules." *AIC Book and Paper Group Annual* 3 (1984): 13-58. 10 December 2023. <https://cool.culturalheritage.org/byauth/burke/solpar/>.

7. Chieh, Chung (Peter). *Hydration*. n.d. 20 December 2023. <https://chem.libretexts.org/Bookshelves/Physical_and_Theoretical_Chemistry_Textbook_Maps/Supplemental_Modules_(Physical_and_Theoretical_Chemistry)/Thermodynamics/Energies_and_Potentials/Enthalpy/Hydration>.

8. Clark, Jim. *COPPER*. July 2015. 30 November 2023. <https://www.chemguide.co.uk/inorganic/transition/copper.html>.

9. Crisponi, Guido, et al. "Kill or cure: Misuse of chelation therapy for human diseases." *Coordination Chemistry Reviews* 284 (2014): 4. 13 December 2023.

10. Daneshfar, Ali, Hassan S. Ghaziaskar and Nasrolah Homayoun. "Solubility of Gallic Acid in Methanol, Ethanol, Water, and Ethyl Acetate." *Journal of Chemical & Engineering Data* 53.2 (2008): 1. 23 December 2023.

11. Edinburgh Instruments. *Techniques: Uv-Vis Spectroscopy*. n.d. 21 December 2023. <https://www.edinst.com/in/techniques/uv-vis-spectroscopy/>.

12. Flora, Swaran J.S. and Vidhu Pachauri. "Chelation in Metal Intoxication." *International journal of environmental research and public health* 7.7 (2010): 2. 13 November 2023.

13. Görgüç, Ahmet, Esra Gençdağ and Fatih Mehmet Yılmaz. "Industrial Pomegranate Wastes and their Functional Benefits in Novel Food Formulations." *Mediterranean Fruits Bio-wastes: Chemistry, Functionality and Technological Applications* (2022): 721. 13 November 2023. <https://link.springer.com/chapter/10.1007/978-3-030-84436-3_31>.

14. Hinck, Ferguson and Puhaakka. "Resistance of EDTA and DTPA to Aerobic Biodegradation." *Water Science & Technology* 35.2-3 (1997): 7. 20 November 2023.

15. Huguenin, Joris, Sidi Ould Saad Hamady and Patrice Bourson. "Monitoring deprotonation of gallic acid by Raman spectroscopy." *Journal of Raman Spectroscopy* 46.11 (2015): 1063-1065. 19 December 2023. <https://analyticalsciencejournals.onlinelibrary.wiley.com/doi/10.1002/jrs.4752>.

16. Kaderides, Kyriakos, Athanasia M. Goula and Konstantinos G. Adamopoulos. "A process for turning pomegranate peels into a valuable food ingredient using ultrasound-assisted extraction and encapsulation." *Innovative Food Science and*

Emerging Technologie 31 (2015): 13. 14 May 2024.

<https://www.sciencedirect.com/science/article/abs/pii/S1466856415001617>.

17. Kupnik, Kaja, et al. "Supercritical Fluid and Conventional Extractions of High Value-Added Compounds from Pomegranate Peels Waste: Production, Quantification and Antimicrobial Activity of Bioactive Constituents." *Plants* 11.7 (2022): 8. 25 December 2023.

18. Lancashire, Robert J. *Stability of Metal Complexes and Chelation*. n.d. 29 November 2023.

<https://chem.libretexts.org/Bookshelves/Inorganic_Chemistry/Supplemental_Modules_and_Websites_(Inorganic_Chemistry)/Coordination_Chemistry/Complex_Ion_Equilibria/Stability_of_Metal_Complexes_and_Chelation>.

19. LibreTexts. "Colors of Coordination Complexes." n.d. *LibreTexts Chemistry.* 6 December 2023.

<https://chem.libretexts.org/Bookshelves/Inorganic_Chemistry/Supplemental_Modules_and_Websites_%28Inorganic_Chemistry%29/Crystal_Field_Theory/Colors_of_Coordination_Complexes>.

20. Lucidchart. *Lucidchart*. n.d. 17 November 2023.

<https://www.lucidchart.com/pages>.

21. Manne, Ravi, et al. "Water quality and risk assessment of copper content in drinking water stored in copper container." *Applied Water Science* 12.3 (2022): 3, 5-6. 22 December 2023.

22. Medina, Enrique. "Methanol Hazards & Safeguards: Lessons Learned From the Global Supply Chain." *Professional Safety* 59.6 (2014): 67–74. 30 May 2024.

<https://onepetro.org/PS/article-abstract/59/06/67/33261/Methanol-Hazards-amp-Safeguards-Lessons-Learned>.

23. Mo, Yaxian, et al. "Pomegranate Peel as a Source of Bioactive Compounds: A Mini Review on Their Physiological Functions." *Frontiers in Nutrition* 9 (2022): 2-3. 17 November 2023.

24. Mokarram, Marzieh, Ali Saber and Vahideh Sheykhi. "Effects of heavy metal contamination on river water quality due to release of industrial effluents." *Journal of Cleaner Production* 277 (2020): 18, 23-24. 19 November 2023.

25. MolView. *MolView*. n.d. 2 December 2023. <https://molview.org>.

26. Muñoz-Muñoz, Jose Luis, et al. "Ellagic acid: Characterization as substrate of polyphenol oxidase." *IUBMB Life* 61.2 (2008): 173-174. 15 December 2023. <https://iubmb.onlinelibrary.wiley.com/doi/full/10.1002/iub.143>.

27. Rashed, Musaab K. and Wissam Tayh. "Removal of Heavy Metals from Wastewater Using Pomegranate Peel." *IOP Conference Series: Materials Science and Engineering* (2020): 1-2. 23 December 2023.

28. Rehman, Kanwal, et al. "Prevalence of Exposure of Heavy Metals and Their Impact on Health Consequences." *Journal of Cellular Biochemistry* (2017): 2. 20 November 2023.

29. Tran, Erica and Dennis Liu. *Solubility and Factors Affecting Solubility*. 30 January 2023. 6 December 2023. <https://chem.libretexts.org/Bookshelves/Physical_and_Theoretical_Chemistry_Textbook_Maps/Supplemental_Modules_(Physical_and_Theoretical_Chemistry)/Equilibria/Solubilty/Solubility_and_Factors_Affecting_Solubility>.

30. U.S. Congress, Office of Technology Assessment. *Copper: Technology and Competitiveness*. Office of Technology Assessment, 1988. 29 November 2023. <https://www.princeton.edu/~ota/disk2/1988/8808/8808.PDF>.

31. United Nations. *Goal 6*. 2022. 16 November 2023. <https://sdgs.un.org/goals/goal6>.

32. Water.org. *An Economic Crisis*. n.d. 17 November 2023. <https://water.org/our-impact/water-crisis/economic-crisis/>.

33. Yoder, Claude H. and Natalie J. Flora. "Geochemical applications of the simple salt approximation to the lattice energies of complex materials." *American Mineralogist* 90.2-3 (2005): 492. 20 December 2023. <https://www.degruyter.com/document/doi/10.2138/am.2005.1537/html>.

34. Zarfeshany, Aida, Sedigheh Asgary and Shaghayegh Haghjoo Javanmard. "Potent health effects of pomegranate." *Advanced Biomedical Research* 3.1 (2014): 1-6. 13 November 2023.

17 Appendix

17.1 Uncertainty calculations for varying CuSO₄ standards

Table 30: Uncertainty calculations for each CuSO$_4$ standard concentration.
The fractional uncertainty of the concentration of the standards are calculated by: $$\frac{\Delta c}{c} = \frac{\Delta m}{m} + \frac{\Delta v}{v}$$
c = metal concentration (moldm^3) | **m** = M$_r$ of CuSO$_4$ | **v** = volume of water added
For 0.025 moldm^{-3}: $$\frac{\Delta c}{0.025} = \frac{0.001}{0.624} + \frac{0.5}{100}$$

$$\Delta c = \pm 1.65 \times 10^{-4}$$

This calculation is repeated for the other standard concentrations:

0.05 moldm^{-3}	$\pm 1.45 \times 10^{-4}$
0.075 moldm^{-3}	$\pm 1.38 \times 10^{-4}$

17.2 Buffer Reagents Preparation

Table 31: Preparation procedure for pH 2 buffer reagents.

16.2.1 Preparation of pH 2 buffer reagents

0.20 moldm^{-3} Hydrochloric Acid Preparation:

Step 1: 1cm^3 of Hydrochloric Acid solution was measured using a pipette then added to 50cm^3 of distilled water in a measuring cylinder.

Step 2: The solution was transferred to a 100cm^3 standard flask and the standard flask was filled with distilled water until the 100cm^3 mark.

0.20 moldm^{-3} Potassium Chloride Preparation:

Step 1: 1.490g of Potassium Chloride was weighed on a digital scale.

Step 2: The salt was then transferred to a beaker containing 50cm^3 distilled water and the solution was stirred thoroughly.

Step 3: The solution was transferred to a 100cm^3 standard flask and the standard flask was filled with distilled water until the 100cm^3 mark.

Table 32: Preparation procedure for pH 5 buffer reagents.

16.2.2 Preparation of pH 5 buffer reagents

0.10 moldm^{-3} Glacial Acetic Acid Preparation:

Step 1: 0.600g of Glacial Acetic Acid was weighed on a digital scale.

Step 2: The salt was then transferred to a beaker containing 50cm^3 distilled water and the solution was stirred thoroughly.

Step 3: The solution was transferred to a 100cm^3 standard flask and the standard flask was filled with distilled water until the 100cm^3 mark.

0.10 moldm^{-3} Sodium Acetate Trihydrate Preparation:

Step 1: 1.362g of Sodium Acetate Trihydrate was weighed on a digital scale.

Step 2: The salt was then transferred to a beaker containing 50cm^3 distilled water and the solution was stirred thoroughly.

Step 3: The solution was transferred to a 100cm^3 standard flask and the standard flask was filled with distilled water until the 100cm^3 mark.